International Journal of Thermophysics, Vol. 22, No. 4, 2001

Water and Gallium at Absolute Negative Pressures. Loci of Maximum Density and of Melting[1]

H. I. M. Veiga,[2] L. P. N. Rebelo,[2,3] M. Nunes da Ponte,[2] and J. Szydlowski[2,4]

Several physical properties of liquids as well as those of the coexistence between liquid and solid can be determined at absolute negative pressures. Examples for this include thermal pressure coefficients, loci of temperature of maximum density, melting lines, speed of propagation of low-intensity sound waves, and (p, T, x) conditions of occurrence of liquid/liquid phase separation. Three model temperature-pressure cycles, which allow for the measurement of temperature-pressure conditions of the occurrence of maxima of liquid density, negatively sloped fusion lines, and the upper critical solution temperature (UCST) of liquid solutions in these metastable regimes are described. A new apparatus for measuring negative pressures was developed. The temperature and pressure are determined within an uncertainty of ± 0.05°C and ± 5 bar, respectively. Water and heavy water have been used as testing systems with respect to the location of their temperatures of maximum density (TMD) loci. Empirical equations of state whose parameters have been fitted to experimental data located in the normal positive pressure region have proven to extrapolate well to the negative pressure regime. Furthermore, an attempt was made to use SAFT in order to provide a more theoretically founded framework. Preliminary results for gallium have shown that a TMD exists 45 K inside the supercooled regime, and that the continuation of its melting line down to -80 bar evolves with a slope of -515 ± 25 bar $\cdot$ K^{-1}.

KEY WORDS: gallium; liquids under tension; maximum density loci; melting line; metastability; negative pressures; water.

[1] Paper presented at the Fourteenth Symposium on Thermophysical Properties, June 25–30, 2000, Boulder, Colorado, U.S.A.

[2] Instituto de Tecnologia Química e Biológica, ITQB 2, Universidade Nova de Lisboa, Apartado 127, 2780-901 Oeiras, Portugal.

[3] To whom correspondence should be addressed. E-mail: luis.rebelo@itqb.unl.pt

[4] Permanent address: Chemistry Department, Warsaw University, Zwirki I Wigury 101, 02-089 Warsaw, Poland.

0195-928X/01/0700-1159$19.50/0

1. INTRODUCTION

Absolute negative pressure regimes constitute a particular case within the more general phenomenon of superheating [1], one in which $p < 0$. Only condensed phases (solid, liquid, liquid–liquid coexistence, or solid–liquid coexistence) can be put under tension at negative pressures. Gases cannot, nor can, obviously, coexistence phases involving a gas phase. Metastability is a relative concept [2]. One must specify with respect to what thermodynamic state a given system is metastable. In order to do so, it is necessary to define the imposed external thermodynamic constraints to the system. The most commonly used constraints are keeping either pressure and temperature (p, T) or total volume and temperature (V, T) constant. In the former case, the totally stable equilibrium state with respect to which the metastable one is referred is found at the minimum of the Gibbs energy. For the latter, i.e., with the volume and temperature held constant, the minimum in the Helmholtz energy determines to which condition of greater stability the system will evolve. Since, for a condensed phase, the act of crossing the $p = 0$ line does not introduce any discontinuity or abrupt change in the physical properties of the system, the most obvious feature of absolute negative pressure regimes in comparison with most cases of metastability (in particular, with superheating at $p > 0$) is that, at $p < 0$, one cannot impose the external constraints of (p, T) = constant. This is because there is no totally stable single phase (or coexistence between phases) at negative pressures. Therefore, in this work, the underlying external constraints when referring to negative pressures are (V, T) = constant.

In spite of their metastability, absolute negative pressure states can be held for considerable periods of time, permitting the measurement of physical properties of substances [3] and their mixtures [4]. Nevertheless, and in contrast with solids, the design of and successful completion of an experiment producing high tension in a liquid are quite difficult [1]. The key factors for success are (i) smoothness and cleanness of the container walls, (ii) absence of gas bubbles and suspended impurities in the liquid, (iii) good adhesion (wettability) between liquid and walls, and (iv) use of the smallest possible amount of liquid sample; the strategy of using several cycles of pressurization/depressurization has also proven useful [5]. Shielding the cell from cosmic rays has also been reported as a possible factor to be taken into account. In the case of isotropic and static production of tension when a liquid phase is present, there are three model experiments (see Figs. 1a–c and their captions) which can lead to the determination of thermodynamic properties at negative pressures. All cases share the use of the Berthelot method [1–5] for generating high tension in a liquid; during an induced isochoric temperature drop of a liquid phase presenting a positive

isobaric expansion coefficient (α_p), the pressure may drop to negative values if nucleation of gas bubbles (cavitation) is avoided. Additionally, the temperature range has to be set below a maximum thermodynamic limit—the intersection of the liquid spinodal with the $p = 0$ line [1]. For anomalous density liquids, the locus of temperature of maximum density (TMD) can be extended to the negative pressure region [3, 6] by performing (p, T) measurements along several distinct isochores (Fig. 1a). For substances with negatively sloped melting lines, the solid–liquid coexistence condition can be monitored (Fig. 1b) at these same regimes [3]. Furthermore, for binary mixtures [4] presenting an upper critical solution temperature (UCST), the phase transition from a homogeneous to heterogeneous region can be induced and detected at negative pressures (Fig. 1c).

The design of reliable experimental studies and an understanding of the behavior of metastable liquids are intellectually challenging. More importantly, over the last few years the importance of metastable liquid studies to the understanding of nontrivial behavior at stable conditions has been demonstrated. Here, liquid water is *the* model system [7], although not an exclusive one [2, 8]. Many open intriguing questions [9], such as whether liquid–liquid metastable phase transitions in pure fluids exist and terminate or not at a metastable critical point, remain to be resolved.

In the present work we briefly describe a new apparatus capable of producing and monitoring absolute negative pressures. We present data for the TMD of H_2O and D_2O (test systems) and, for the first time, the continuation below zero pressure of the negatively sloped melting curve of gallium(I), as well as a point of the locus of its TMD in the simultaneous supercooled and stretched region. Methanol, a substance with no special anomalies, has also been investigated for comparison purposes. It should be emphasized that the $T-p$ range of our experimental measurements is well removed from the thermodynamic limit of mechanical stability [1, 2]—where the response functions such as isothermal compressibility, isobaric thermal expansion, and heat capacity diverge—the spinodal line. Our methodology does not at all seek to search for that limit, rather it aims to measure physical properties in metastable regimes well removed from it. The "end-point" of the experiments described herein—the collapse of the system—is due to heterogeneous nucleation of the stable phase(s), which is a kinetic interfacial phenomenon. It is not provoked by enhanced bulk density fluctuations that occur near the mechanical limit of stability.

We have also tested the ability of empirical equations of state to reproduce experimental data of liquid isochores in this metastable region. Finally, more theoretically founded equations of state such as the statistical associating fluid theory (SAFT) [10] are discussed.

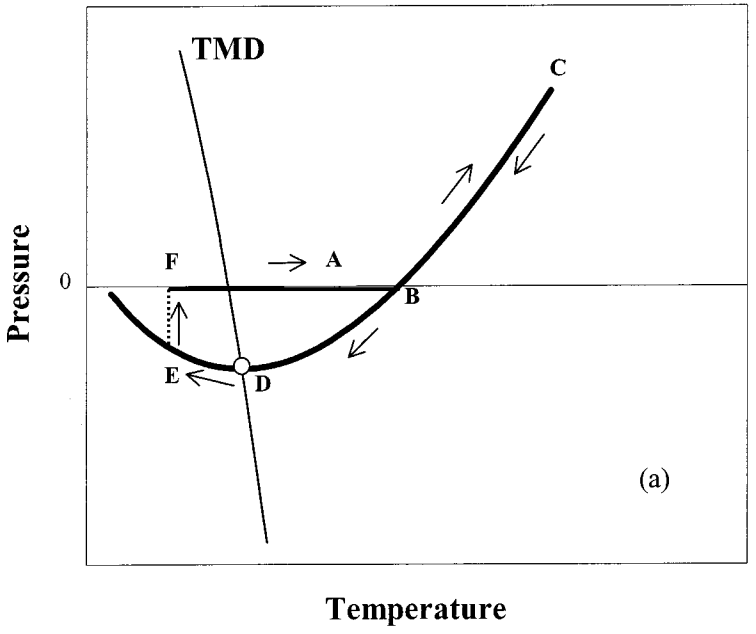

Fig. 1. Schemes of cycles of temperature-pressure in Berthelot-type experiments. Thick lines: course of the experiment; thin lines and circles: relevant property to be determined. (a) TMD: A-B, warming process along the vaporization line; due to expansion, at B the liquid occupies the whole volume of the container; B-C, expansion continues at a much higher rate along an isochore; on reversing the process (C-B-D) by cooling, the liquid starts to be under tension at B; in the case of substances showing TMD (where $\alpha_p = 0$), the liquid starts to expand on cooling between D-E; at E the liquid may collapse and relax to the stable condition (F). (b) T_M: A-B-C, cooling process along the vaporization line; B-C, supercooled liquid–gas regime; C, solidification is triggered; in the case of substances showing a negatively sloped melting line, this solidification corresponds to a sudden increase of pressure (C-D); D-E, isochoric warming of solid; fusion starts at E with contraction; at F the system may collapse, relaxing to the stable condition (G). (c) UCST: everything is similar to (a), but the isochore crosses now the phase separation border.

The choice of gallium as a substance of study arose from the belief that a close interrelationship exists between liquid density anomalies, negatively sloped melting curves, and open molecular coordination environments. Liquids with such characteristics are also good candidates for demonstrating liquid–liquid coexistence, which may develop either in the more experimentally accessible stable region or in the more hidden metastable one.

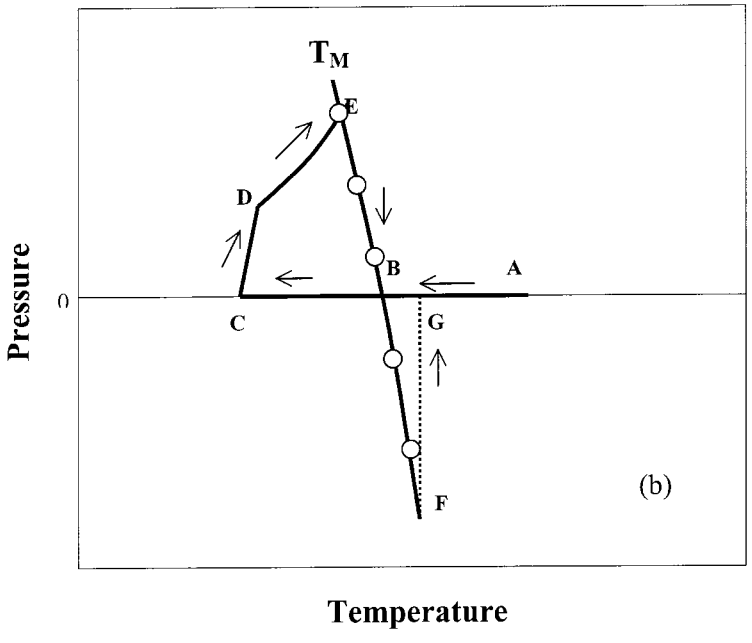

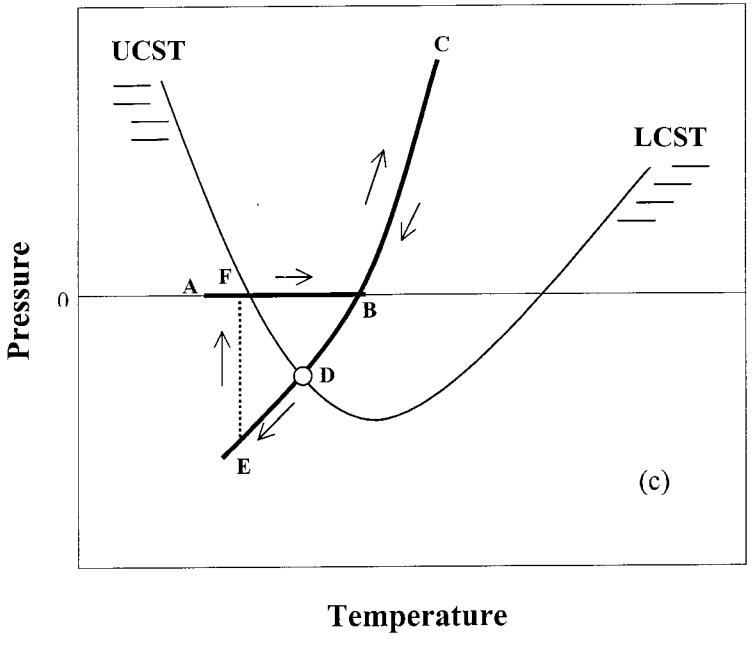

Fig. 1. (*Continued*)

2. EXPERIMENTAL

The experimental setup is similar to one previously reported by Speedy [3, 11], but contains several modifications. We have manufactured the glass capillary helixes from normal Pyrex glass tubing. Each tube was stretched under heat, wound around a graphite cylinder under a flame, and etched in 5% aqueous solution of HF for several minutes. Typical I.D.'s and O.D.'s of initial helixes (before etching) are 0.12 ± 0.02 mm and 0.24 ± 0.02 mm, respectively. Final internal volumes, V_{int}, are within the range $0.002\ \text{cm}^3 < V_{\text{int}} < 0.004\ \text{cm}^3$. The helixes act simultaneously as Berthelot tubes and Bourdon spiral gages. The major improvement in comparison with Speedy's apparatus lies in temperature control and measurement. The glass helix is suspended inside a stainless steel (SS) cell with a large glass window. The SS cell can be evacuated for temperature control or filled with helium (300 mbar) to produce temperature changes. In turn, the SS cell is immersed in a thermostated (better than 0.01 K) bath, which also has a large glass window. A four-wire PRT (100 Ω, readable to 0.001 K) monitors the temperature of the bath. Additionally, a copper/constantan thermocouple detects any temperature difference between the external bath and the interior of the cell in close proximity to the helix. Deflection of the glass helix due to the fluid pressure is measured by the change in position of a HeNe laser beam, reflected off of a mirror attached to the bottom of the helix, and imaged on a large curved screen about 3 m from the cell.

The pressure uncertainty is estimated to be ± 5 bar, judging from the standard deviation of the pressure calibration curves.

The water used in this work was double distilled, deionized (Millipore equipment), degassed using a vacuum line, and filtered (Chromofil disks of 0.20 μm porosity from Mackercy–Nagel) from suspended impurities prior to injection into the glass helix. D_2O was purchased from Chemika–Fluka with a claimed isotopic purity of 99.8 atom% D, and it was only further degassed and filtered similar to normal water. Methanol (Aldrich Chemical Co., 99.8% purity) was cryogenically degassed and filtered. Gallium (Aldrich Chemical Co., chemical purity 99.9999%) was used as received. In order to maintain it in the liquid state, gallium had to be injected into the glass helix while inside a specially designed transparent acrylic oven operating at about 40°C (m.p. of Ga(I) = 29.78°C).

3. RESULTS AND DISCUSSION

We have searched for the TMD of H_2O and D_2O in order to test our new apparatus and methodology. Data for the quasi-isochores for each system are represented in Figs. 2a and 2b. Note that it was possible not

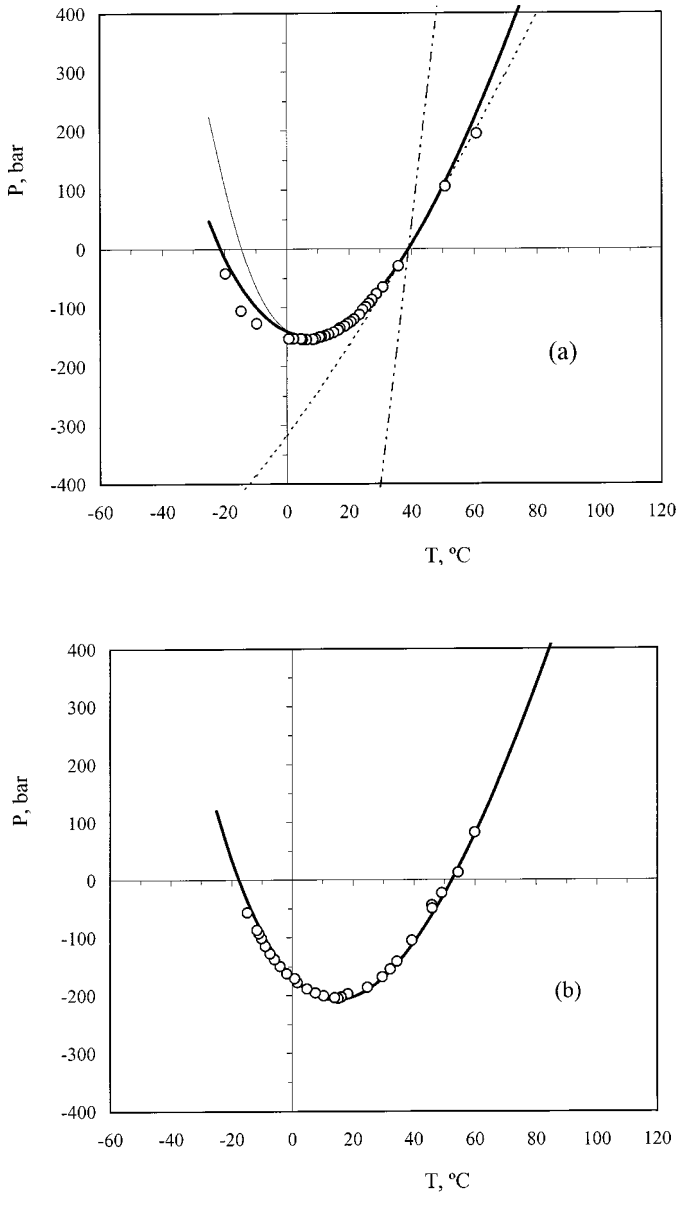

Fig. 2. $p-T$ curves for water. (a) H_2O: (○) experimental data from this work at $\rho \cong 0.99256\ g \cdot cm^{-3}$; (——) from Chen et al. [14]; (—) from Speedy [13]; dotted and dotted-dashed lines from SAFT [10] (see text). (b) D_2O: (○) experimental data from this work at $\rho \cong 1.09476\ g \cdot cm^{-3}$; (——) from Fine and Millero [15].

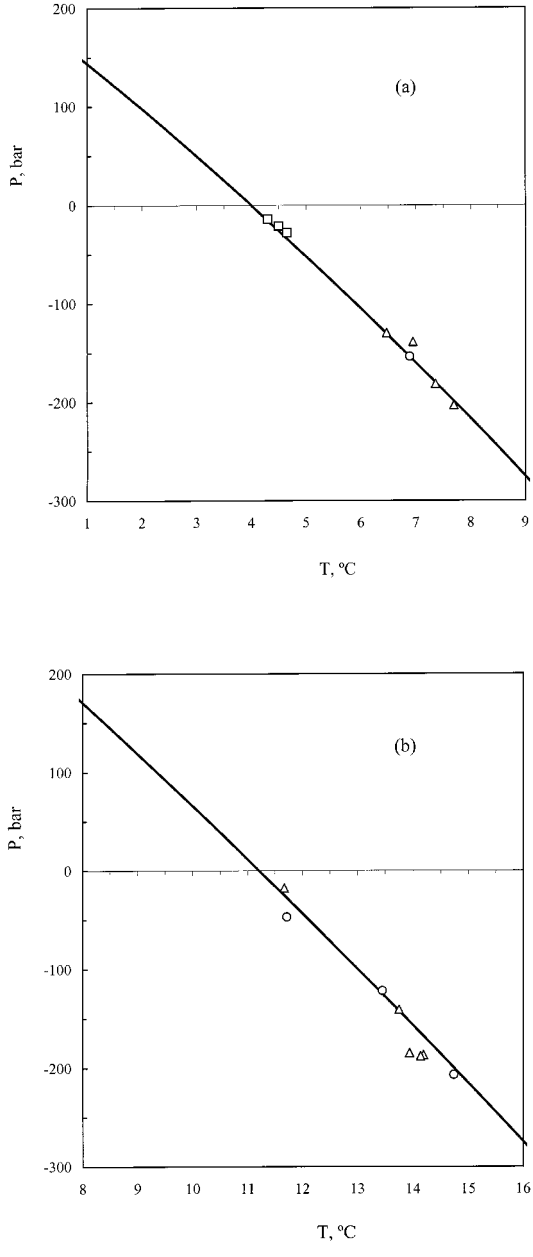

Fig. 3. TMD of water at negative pressure. (○), this work; (△), from Ref. 3; (□), from Ref. 12; (——), EoS: in (a), Ref. 14 for H_2O, in (b) Ref. 15 for D_2O.

only to maintain liquid water in the negative pressure regime, but also to supercool it to $-20°C$ and $-15°C$ in the cases of normal and heavy water, respectively. Below their triple point temperatures and sublimation pressures, liquid water is in a doubly metastable condition with respect to the solid and gas phases. Strictly speaking, the minimum of each experimental quasi-isochore does not coincide with the location of the TMD. This is obviously due to the non-zero values of both the thermal expansivity and isothermal compressibility of the glass helix. For those minima conditions, estimated corrections taking these effects into account have proven to be of the size of the overall temperature and pressure uncertainties of the experiment, typically $\pm 0.05°C$ and ± 5 bar, respectively. Figures 3a and 3b compare our results for the TMDs at negative pressures with other data available in the literature [3, 12] and with extrapolated predictions to this region of commonly used equations of state (EoS) [13–15]. In both cases, the agreement is good. Our experimental points in each case locate the TMD of H_2O at (6.89°C, −153.7 bar) and that of D_2O at (11.71°C, −46.8 bar; 13.45°C, −121.9 bar; 14.74°C, −206.7 bar). Figure 4 shows a typical

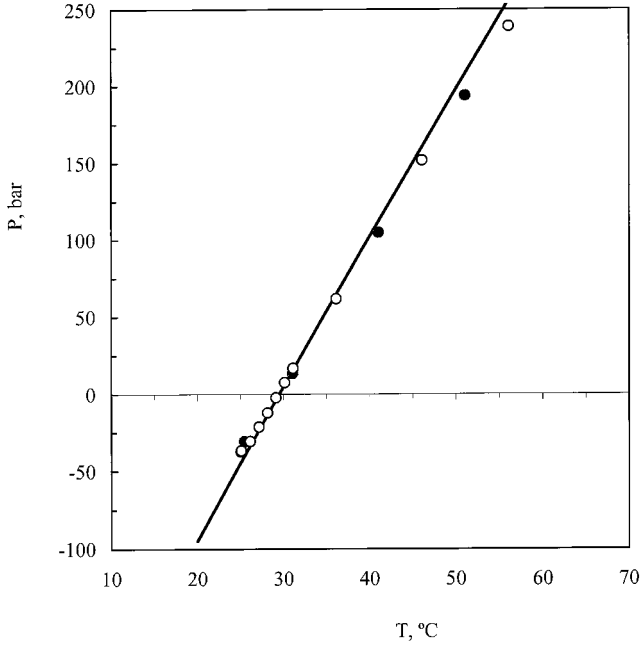

Fig. 4. $p-T$ curve for methanol at $\rho \cong 0.78242\ g \cdot cm^{-3}$. Two sets of experimental data (○, ●) are represented; (——) from Machado and Streett [16].

Table I. $p - T$ Values of Quasi-Isochores for Three Liquids Under Positive and Negative Pressure (Experimental Data Represented in Figs. 2a, 2b, and 4)

T (°C)	P (bar)
H_2O ($\rho \cong 0.99256\ g \cdot cm^{-3}$)	
60.75	195
35.81	−29.5
30.82	−65.3
28.81	−76.8
27.34	−86.7
26.33	−93.3
25.33	−99.0
24.35	−104
23.36	−112
21.56	−121
20.59	−125
19.58	−128
18.53	−132
17.06	−135
16.51	−139
15.05	−142
13.46	−146
12.28	−148
11.08	−150
10.47	−151
9.14	−153
8.37	−154
6.31	−155
5.01	−153
4.46	−151
2.16	−150
0.65	−148
−4.43	−135
−9.69	−121
−14.73	−98.2
−19.74	−29.5
D_2O ($\rho \cong 1.09476\ g \cdot cm^{-3}$)	
59.87	82.1
54.52	12.6
49.14	−23.4
45.9	−44.1
46.00	−52.0

Table I. *(Continued)*

T (°C)	P (bar)
39.36	−108
34.47	−143
32.29	−157
29.68	−170
24.78	−189
18.33	−204
16.18	−208
15.20	−208
14.02	−207
10.40	−204
7.67	−197
4.89	−189
1.70	−175
0.81	−171
−1.77	−161
−4.02	−146
−5.82	−134
−7.33	−122
−8.88	−109
−10.14	−95.9
−10.99	−87.5
−11.62	−78.5
−14.81	−35.7
CH_3OH ($\rho \cong 0.78242\ g \cdot cm^{-3}$)	
(set # 1)	
51.07	194
41.05	105
31.07	13.4
25.47	−30.7
25.02	−37.3
(set # 2)	
56.10	238
46.10	152
36.13	61.6
31.14	16.7
30.14	7.5
29.12	−2.3
28.15	−12.1
27.15	−21.4
26.12	−30.7
25.08	−36.7

isochore for methanol. As expected, liquid methanol always (ten trials, only two are shown) collapsed at a lower (negative) tension (highest tension of about -40 bar) in comparison with water. This is due to the weaker adhesion of methanol to glass (heterogeneous nucleation). In all cases, it should be emphasized how well empirical EoS [14–16], whose parameters have been fitted to experimental data available at positive pressures, can quantitatively predict the continuation of the TMDs and/or of isochores, at least down to -200 bar. Experimental data of the quasi-isochores of H_2O, D_2O, and methanol, represented in Figs. 2a, 2b, and 4, respectively, are reported in Table I.

This fact has also motivated us to test less empirical EoS. The statistical associating fluid theory (SAFT) has been one of the most widely used and successful equations of state [10]. It is founded on a molecular basis and is appropriate for studying the behavior of strongly associated fluids and their mixtures, including those with hydrogen bonds. We have used its hard-sphere (HS) version [10]. We were interested to see whether the same theory could also shed some light on the origin of still controversial interpretations of the abnormal features of supercooled water [9, 17]. We refer to the apparent divergences in response functions such as compressibility (K_T), expansivity (α_p), and heat capacity (C_p), and the possible existence of a metastable liquid–liquid critical point. Nonetheless, and a bit surprisingly, the results obtained have proven that SAFT-HS could not be used for such purposes.

Figure 2a shows the SAFT-HS isochore which was obtained for the experimental run at $\rho = 0.99256\ \mathrm{g \cdot cm^{-3}}$. This is the experimental orthobaric density of H_2O at $T = 39.15°C$. In turn, this temperature is set as the one at which the vapor pressure of water curve intersects our isochoric experimental results (filling temperature). Using the proposed model parameters [10] for SAFT-water fitted at its critical point ($\sigma = 3.099 \times 10^{-10}$ m; $e^{\mathrm{mf}}/k = 4642$ K, and $e^{\mathrm{hb}}/k = 1625$ K) one gets the dotted-dashed curve represented in Fig. 2a. In fact, in order to get total agreement between the above mentioned filling temperature and corresponding orthobaric density, we have slightly changed $\varepsilon^{\mathrm{hb}}/k$ to 1688 K. Note the large disagreement between the theoretical and experimental isochores, even in the totally stable regime. Moreover, we were unable to find in SAFT-water any isochore within the liquid range (stable and metastable) showing any minimum, therefore, no TMD, independently of the values of all three parameters within a large range of variation. For example, the best fit to our experimental isochore in the vicinity of the filling temperature (dotted curve in Fig. 2a) has been obtained with $\sigma = 2.67 \times 10^{-10}$ m, $e^{\mathrm{mf}}/k = 916$ K, and $e^{\mathrm{hb}}/k = 1688$ K. The corresponding reduced density variation is from $\eta = 0.517$ to 0.33. The slope of the $p - T$ curve at that filling temperature now agrees with experiment

but diverges from it in any other region. This slope is simply the thermal pressure coefficient,

$$\gamma_v = (\partial p/\partial T)_v = -(\partial V/\partial T)_p/(\partial V/\partial p)_T = \alpha_p/K_T \tag{1}$$

We have also been unable to find other well identified characteristics of water such as the locus of minima in the temperature dependence of K_T, which occurs in the totally stable region of the phase diagram. The conclusion is that, while the critical point and coexistence line are relatively well predicted by SAFT for water, its compressibility and expansivity, and, thus, much of the abnormal behavior at normal conditions, are not. Results have shown that SAFT is inadequate to describe such peculiarities of anomalous density liquids as oriented medium-range interactions. Other failures of SAFT have recently been reported by other authors [18]. No serious criticism of SAFT is intended here. Instead, we merely caution against its blind application.

We now turn our attention to gallium. Preliminary results have shown that we have detected a point of the locus of maximum density of liquid gallium in the supercooled and stretched (-200 bar) regime at about 45 K deep inside this metastable region. Experiments to determine the slope of this metastable TMD are currently in progress. It has long been known that gallium is much easier to undercool than water. The continuation to negative pressures of the melting curve of gallium(I) was also investigated. Crystallization is hard to achieve, and in order to perform an experiment similar to that schematically sketched in Fig. 1b, we had to immerse one end of the glass helix in liquid nitrogen (point C) as a seeding procedure to trigger solidification. Then, the full process of solidification inside the helix took about 0.5 h. Further warming (portion D-E of Fig. 1b) has revealed a thermal pressure coefficient in the solid, $\gamma_v = 29 \pm 1$ bar $\cdot$ K^{-1}. Figure 5 shows a first set of experimental data during melting obtained between c.a. -80 and 180 bar. More experimental sets of data are being undertaken. As fusion proceeds, the liquid, the solid, and the liquid–solid interface are put under tension due to contraction [19] ($\Delta^f V/V = -0.031$). The experimental slope of the melting line between those two pressures is

$$(dp/dT)_f = \Delta^f S/\Delta^f V = \Delta^f H/(T_f \Delta^f V) = -515 \pm 25 \text{ bar} \cdot \text{K}^{-1} \tag{2}$$

to be compared with a fitted value [20] obtained from data [21] at a high positive pressure of -475 ± 75 bar $\cdot$ K^{-1}. Jayaraman et al. [22] report a value of -500 bar $\cdot$ K^{-1} at 1 bar, which is in better agreement with our data. It should be noted that our temperature scale has been slightly shifted

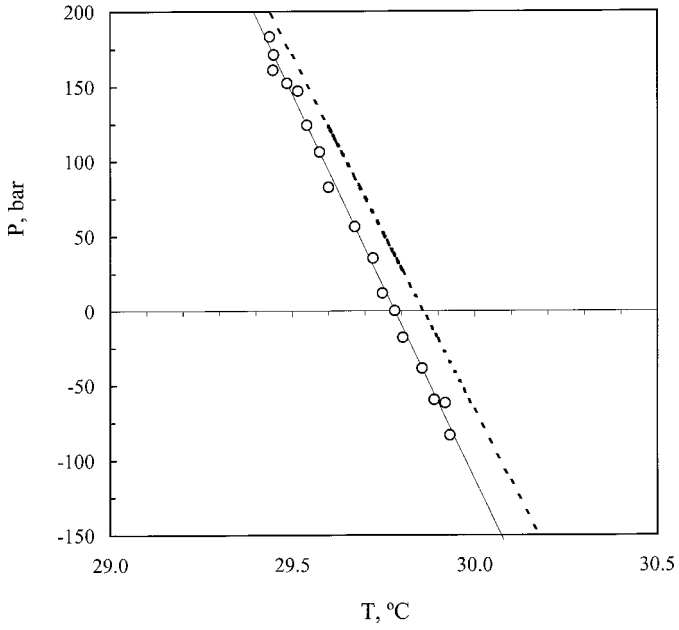

Fig. 5. Melting curve of gallium(I) at positive and negative pressures. (○) experimental, this work; thin line is a least-squares fitting to our data; thick dashed line, from Ref. 22.

in order to reproduce the literature melting point [23] of gallium of 29.78 ± 0.01°C at atmospheric pressure.

Tetrahedral liquids are potential candidates for featuring density anomalies [8]. Gallium has an open structure, though not tetrahedral. Solid Ga(I) possesses a unique orthorhombic structure [22, 24] in which each atom has only one nearest neighbor, with six other ones farther away ("Ga_2 molecules"). The corresponding effective pair potential is rather peculiar [24]. This complex structure is surely responsible for the increase in density upon melting as well as its strong tendency to supercool below the freezing point, and its anomalously long liquid range. Consequently, gallium is also a good candidate for exhibiting a liquid–liquid phase transition and a TMD locus. The latter has recently been detected in a preliminary run performed in this work.

4. CONCLUSIONS

Tension was successfully applied to liquid normal and heavy water, methanol, and gallium down to absolute negative pressure regimes. A new

apparatus was conceived in order to permit a direct determination of those negative pressure values. Its reliability was checked by comparison of our original data against interpolated literature data for both water systems. Novel data for methanol and gallium were also presented. In the case of gallium we were able to extend its melting line down to -80 bar, and a point of its locus of maximum density in the hidden doubly metastable state was detected. Further developments should include the determination of the slope of the TMD of gallium as well as the underlying links between its existence and the liquid structure of this element.

ACKNOWLEDGMENTS

HIMV and JS are grateful to *PRAXIS* (BD/3958/94 and BCC/16424/98, respectively). This work was financially supported by *PRAXIS* under Contract #2/2.1/QUI/178/94.

REFERENCES

1. A. Imre, K. Martinás, and L. P. N. Rebelo, *J. Non-Equilib. Thermodyn.* **23**:351 (1998).
2. P. G. Debenedetti, *Metastable Liquids* (Princeton Univ. Press, Princeton, New Jersey, 1996).
3. S. J. Henderson and R. J. Speedy, *J. Phys. Chem.* **91**:3062 (1987); S. J. Henderson and R. J. Speedy, *J. Phys. Chem.* **91**:3069 (1987).
4. A. Imre and W. A. Van Hook, *J. Polym. Sci. B Polym. Phys.* **32**:2283 (1994); A. Imre and W. A. Van Hook, *Chem. Soc. Rev.* **27**:117 (1998).
5. Y. Ohde, M. Ikemizu, H. Okamoto, W. Hosokawa, and T. Ando, *J. Phys. D Appl. Phys.* **21**:1540 (1988); Y. Ohde, H. Watanabe, K. Iro, K. Motoshita, and Y. Tanzawa, *J. Phys. D Appl. Phys.* **26**:1188 (1993).
6. Q. Zheng, D. J. Durben, G. H. Wolf, and C. A. Angell, *Science* **254**:829 (1991).
7. R. J. Speedy and C. A. Angell, *J. Chem. Phys.* **65**:851 (1976); R. J. Speedy, *J. Phys. Chem.* **86**:982 (1982); C. M. Sorensen, *Nature* **360**:303 (1992); R. J. Speedy, *Nature* **380**:289 (1996); P. G. Debenedetti, *Nature* **392**:127 (1998); O. Mishima and H. E. Stanley, *Nature* **396**:329 (1998); S. Sastry, *Nature* **398**:467 (1999); H. E. Stanley, S. V. Buldyrev, M. Canpolat, O. Mishima, M. R. Sadr-Lahijany, A. Scala, and F. W. Starr, *Phys. Chem. Chem. Phys.* **2**:1551 (2000).
8. P. H. Poole, T. Grande, C. A. Angell, and P. F. McMilan, *Science* **275**:322 (1997); Y. Katayama, T. Mizutani, W. Utsumi, O. Shimomura, M. Yamakata, and K.-I. Funakoshi, *Nature* **403**:170 (2000); C. A. Angell, R. D. Bressel, M. Hemmati, E. J. Sare, and J. C. Tucker, *Phys. Chem. Chem. Phys.* **2**:1559 (2000); H. Maris and S. Balibar, *Physics Today Web Ed.*, http://www.aip.org/pt/feb00/maris.htm (2000).
9. L. P. N. Rebelo, P. G. Debenedetti, and S. Sastry, *J. Chem. Phys.* **109**:626 (1998).
10. A. Galindo, P. J. Whitehead, G. Jackson, and A. N. Burgess, *J. Phys. Chem.* **100**:6781 (1996); D. G. Green and G. Jackson, *J. Chem. Soc. Faraday Trans.* **88**:1395 (1992).
11. S. J. Henderson and R. J. Speedy, *J. Phys. E Sci. Instrum.* **13**:778 (1980).
12. J. Meyer, *Abh. Dtsch. Bunsen. Ges.* **6**:1 (1911).
13. R. J. Speedy, *J. Phys. Chem.* **86**:982 (1982).

14. C.-T. Chen, R. A. Fine, and F. J. Millero, *J. Chem. Phys.* **66**:2142 (1977).
15. R. A. Fine and F. J. Millero, *J. Chem. Phys.* **63**:89 (1975).
16. J. R. S. Machado and W. B. Streett, *J. Chem. Eng. Data* **28**:218 (1983).
17. S. Sastry, P. G. Debenedetti, F. Sciortino, and H. E. Stanley, *Phys. Rev. E* **53**:6144 (1996).
18. N. Koak, T. W. de Loos, and R. A. Heidemann, *Ind. Eng. Chem. Res.* **38**:1718 (1999).
19. *Handbook of Chemistry and Physics*, 53rd ed., R. C. Weast, ed. (CRC Press, Cleveland, Ohio, 1972).
20. S. E. Babb Jr., *Rev. Mod. Phys.* **35**:400 (1963).
21. P. W. Bridgman, *Proc. Am. Acad. Arts Sci.* **56**:61 (1921).
22. A. Jayaraman, W. Klement, Jr., R. C. Newton, and G. C. Kennedy, *J. Phys. Chem. Solids* **24**:7 (1963).
23. G. B. Adams, Jr., H. L. Johnston, and E. C. Kerr, *J. Am. Chem. Soc.* **74**:4784 (1952); E. B. Amitin, Y. F. Minenkov, O. A. Nabutovskaya, I. E. Paukov, and S. I. Sokolova, *J. Chem. Thermodyn.* **16**:431 (1984).
24. D. A. Young, *Phase Diagrams of the Elements* (Univ. California Press, Berkeley, California, 1991).